

Thermal decomposition of pure and rhodium impregnated cerium(III) carbonate hydrate in different atmospheres

Celestino Padeste^a, Noel W. Cant^b and David L. Trimm^{a,1}

^a *School of Chemical Engineering and Industrial Chemistry, University of New South Wales, PO Box 1, Kensington, NSW 2033, Australia*

^b *School of Chemistry, Macquarie University, NSW 2109, Australia*

Received 19 June 1993; accepted 15 October 1993

The thermal decomposition of pure and rhodium impregnated cerium(III) carbonate hydrate in oxidising, reducing and inert atmospheres has been studied using combined thermogravimetry/mass spectrometry (TG/MS) and X-ray photoelectron spectroscopy (XPS). In oxygen, the decomposition of the pure carbonate proceeds in two steps, yielding H₂O, CO₂, and cerium(IV) oxide. In inert or reducing atmospheres, the second decomposition step is shifted towards higher temperatures and is divided into two parts. In the second part, CO₂ evolved is partly reduced by Ce(III) to CO and to elemental carbon, and non-stoichiometric CeO_{2-x} is formed as the solid product. In the presence of rhodium as a reduction catalyst, decomposition in helium yields hydrogen and less carbon monoxide than that of the pure carbonate, due to the water–gas shift activity of the solid. In hydrogen, quantitative reduction of the carbon dioxide evolved to methane and water is observed when rhodium is present.

Keywords: Atmospheric control of carbonate decompositions; reduction of carbon oxides by Ce(III); reduction of carbon oxides by H₂ over Rh/ceria

1. Introduction

Carbonates are widely used as precursors for metal-oxide systems used as catalysts, semiconductors or as ceramic high temperature superconductors. Oxides made from pure or doped cerium carbonates are interesting because of their ionic conductivity [1] which makes them applicable as oxygen sensors or electrode materials in fuel cells. Ionic conductivity is also an interesting property of a solid used as a catalyst support material.

In carbonate decomposition reactions, the surrounding atmosphere as well as admixed catalytically active metals may play a very important role in determining

¹ To whom correspondence should be addressed.

the characteristics of the solid products as well as the distribution of volatile products. It has been reported that, during the decomposition of alkaline earth carbonates under atmospheric pressure of hydrogen, the CO_2 evolved is reduced to CO for pure carbonates, and to CH_4 in the presence of hydrogenation catalysts [2–4]. The decomposition temperatures are also considerably lower in the presence of hydrogen as compared to inert atmospheres, a fact that influences the physical and chemical properties of the solid products [3,5].

One particularly interesting system is the interaction between rhodium and cerium salts. Rhodium is added to car exhaust catalysts to catalyse the reduction of nitrogen oxides to nitrogen [6]. Ceria is added to the catalyst originally to provide a source of oxygen for fuel rich excursions in the exhaust gases [7], although this role has been questioned in recent years. Rhodium–ceria interactions appear to be more important in determining catalytic activity [6,8], but little is known about the nature of such interactions.

Compared to most other carbonates, cerium(III) carbonates take a special position because the “ Ce_2O_3 ” theoretically left after removal of CO_2 and H_2O is a very strong reducing agent. In the Ce/O system, CeO_2 is the thermodynamically stable oxide down to very low partial pressures of oxygen, because the oxidation state +IV of cerium ions is very well stabilised in the fluorite type CeO_2 structure. Ce_2O_3 or nonstoichiometric CeO_{2-x} produced as intermediate of carbonate decompositions provides an “internal” reduction source for CO_2 or H_2O . Similar situations are known for decompositions of FeCO_3 or CoCO_3 , during which oxidation of Fe^{2+} and Co^{2+} are likely to occur [9].

Most studies reported on decomposition reactions of cerium(III) carbonates have been carried out in air [1,10]. Under these conditions, Ce(III) is oxidised by molecular oxygen and CO_2 and H_2O are evolved unreduced. Investigation of the decompositions of $\text{Ce}_2(\text{CO}_3)_3 \cdot 8\text{H}_2\text{O}$ and $\text{Ce}(\text{OH})\text{CO}_3 \cdot x\text{H}_2\text{O}$ in the absence of oxygen have been reported by Peterson et al. [11]. The experiments, carried out in a closed pressure vessel in the temperature range 400–700°C, revealed quantitative oxidation of the cerium to CeO_2 by CO_2 and H_2O evolved from the carbonates. CO, H_2 and traces of CH_4 were detected in the product gas mixtures [11]. Since the reactions were performed in a closed system, product analysis was only possible in the final stage of the decompositions. The experiments did not provide much information on the decomposition and reduction/oxidation sequences. The present studies are focused on these issues for both pure and rhodium impregnated cerium carbonate hydrate.

2. Experimental

Cerium(III) carbonate hydrate (Aldrich, 99.9%) was used for the investigations on the pure carbonate. The stoichiometry of the substance was

$\text{Ce}_2(\text{CO}_3)_3 \cdot 4.5\text{H}_2\text{O}$, as assessed from the weight loss and the distribution of volatile products formed during thermal decomposition in oxygen.

The Rh impregnated sample was prepared by adding 2.7 g of the pure carbonate (= 10 mmol of Ce) to a solution of 42 mg (0.2 mmol) of rhodium chloride in 20 ml distilled water. After stirring at room temperature for 30 min and evaporation of the water at 90°C, the solid was dried at 150°C overnight.

The thermal decomposition of pure and impregnated carbonates were studied using a Setaram 111 thermomicrobalance/microcalorimeter (TG/DSC). In each experiment, between 25 and 35 mg of sample was placed in a platinum crucible and heated linearly at 10°C/min from room temperature to 800°C in a flow of 50 to 100 ml/min of either helium, oxygen or hydrogen. Gases evolved during the decompositions were analysed using a Balzers GAM 400 mass spectrometer, which was coupled to the outlet of the TG/DSC.

The XPS spectra were recorded on a Kratos XSAM AXIS 800 pci spectrometer equipped with a concentric hemispherical analyzer which was run in the fixed transmission mode at pass energy 40 eV. A Mg K_α X-ray source was used at 180 W. The base pressure of the system was less than 10^{-9} Torr. The energy scale of the spectra of non-conducting samples was calibrated against the C 1s line of adventitious carbon at $E_B = 284.6$ eV. The samples were ground to fine powders and suspended in acetone. The resulting slurry was deposited on a stainless steel sample holder. After evaporation of the solvent, the powder was bound to the holder sufficiently strongly to be introduced in the vacuum system. Thermal pretreatments of the samples in vacuum (less than 10^{-4} Torr) or flowing oxygen at ambient pressure were performed in a chamber attached to the spectrometer. The treated samples were then transferred to the main chamber of the instrument without contact with air.

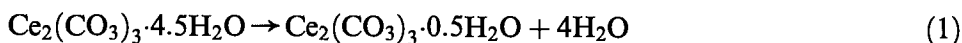
3. Results and discussion

3.1. THERMOGRAVIMETRY/MASS SPECTROMETRY

3.1.1. Decomposition of pure cerium carbonate hydrate in oxygen

Fig. 1 shows that the thermal decomposition of the pure cerium carbonate hydrate under oxygen proceeds in two steps. In a first strongly endothermic step water alone is evolved between 80 and 190°C. The weight loss corresponds to about 4 H_2O per formula unit. The remaining crystal water is evolved concurrently with the production of 3 CO_2 per formula unit in a second step between 190 and 350°C. The relatively small peak in the $m/e = 28$ curve is due to the fragmentation of CO_2 in the mass spectrometer, and not to formation of carbon monoxide during the decomposition.

The decomposition sequence of the carbonate in oxygen can then be written as



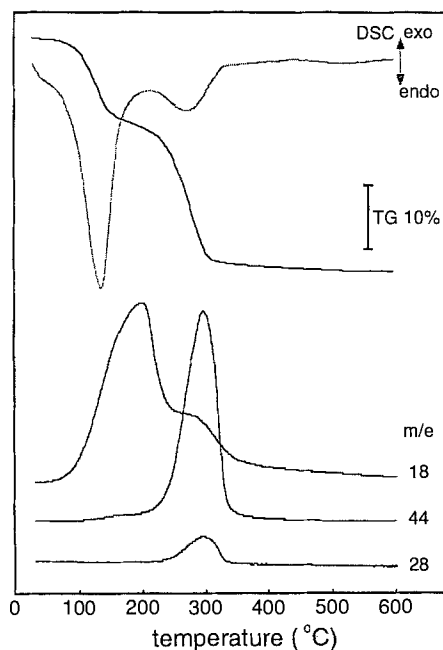
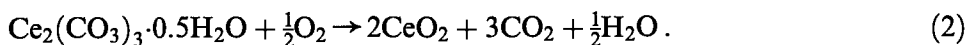


Fig. 1. Thermal decomposition of 30 mg $\text{Ce}_2(\text{CO}_3)_3 \cdot 4.5\text{H}_2\text{O}$ in oxygen. Heating rate: $10^\circ\text{C}/\text{min}$, detected gases: H_2O ($m/e = 18$), CO_2 ($m/e = 44$) and CO ($m/e = 28$). The peak in the $m/e = 28$ curve is due to fragmentation of CO_2 in the mass spectrometer and not to formation of CO during the reaction.



A comparison of theoretical and experimental weight losses of the two decomposition steps is given in table 1.

The only slightly endothermic character of reaction (2) is surprising for a carbonate decomposition, but can be explained in terms of the exothermic oxidation of Ce(III) by O_2 to Ce(IV), which takes place simultaneously. ΔH values at 298 K for reactions involved in decompositions of $\text{Ce}_2(\text{CO}_3)_3 \cdot 4.5\text{H}_2\text{O}$ are summarized in table 2.

Table 1
Theoretical and experimental weight losses during decomposition of $\text{Ce}_2(\text{CO}_3)_3 \cdot 4.5\text{H}_2\text{O}$ in oxygen

Reaction	Temperature of decomposition ($^\circ\text{C}$)	Weight loss (%)	
		theoretical	experimental
(1)	50–190	13.3	13.3
(2)	190–500	23.1	22.9

Table 2

ΔH values at 298 K for reactions involved in decompositions of $\text{Ce}_2(\text{CO}_3)_3 \cdot 4.5\text{H}_2\text{O}$ calculated from literature values for parent materials and products [12,13]

Reaction	ΔH (kcal/mol)
loss of 1 CO_2 from cerium carbonate	20–30 ^a
$\text{CeO}_{1.5} + \frac{1}{4}\text{O}_2 \rightarrow \text{CeO}_2$	-42.6
$\text{CeO}_{1.5} + \frac{1}{2}\text{CO}_2 \rightarrow \text{CeO}_2 + \frac{1}{2}\text{CO}$	-8.8
$\text{CO}_2 + 4\text{H}_2 \rightarrow \text{CH}_4 + 2\text{H}_2\text{O}$	-39.8
$\text{CO} + 3\text{H}_2 \rightarrow \text{CH}_4 + \text{H}_2\text{O}$	-49.4

^a Estimated from values for MgCO_3 and FeCO_3 .

3.1.2. Decomposition of cerium carbonate hydrate in hydrogen and helium

The decompositions of the pure carbonate in helium and hydrogen are very similar (fig. 2) with the steps slightly less resolved than during decomposition in oxygen. The first step involves loss of 4 H_2O , analogous to the decomposition in oxygen. The loss of the last $\frac{1}{2}\text{H}_2\text{O}$ occurs in a further endothermic step around 300°C. The evolution of traces of CO_2 starts at the same temperature, but the maximum decomposition rate is not reached until 480°C. The final decomposition step is divided into two parts with a weight loss ratio of about $\frac{2}{3} : \frac{1}{3}$. In the first part, CO_2 is evolved. For the decomposition in hydrogen, formation of small amounts

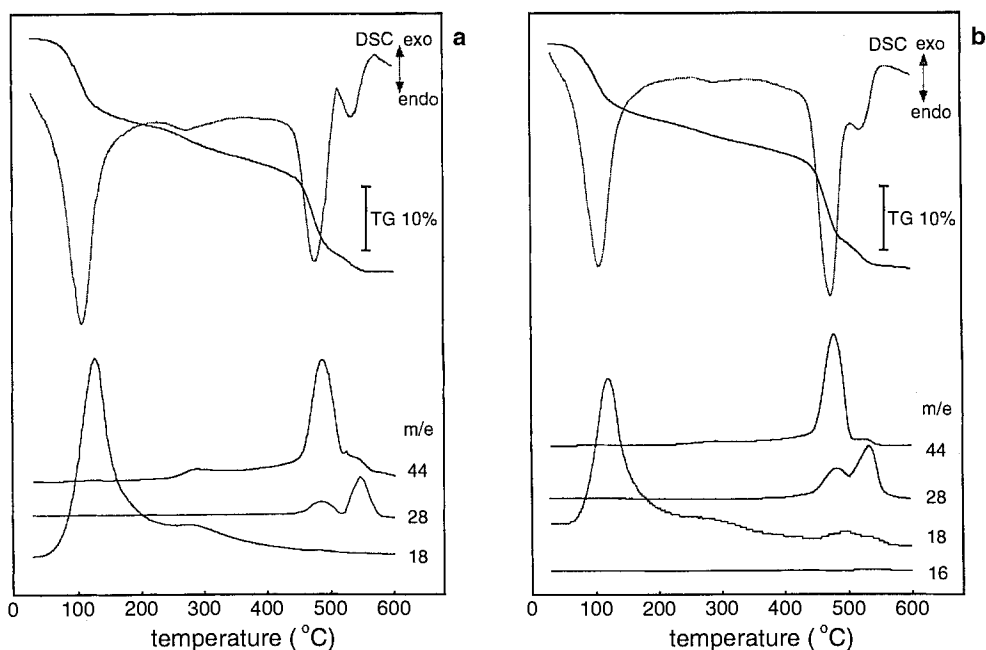
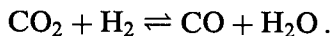


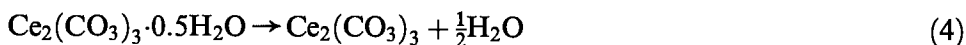
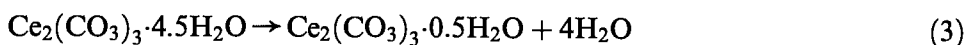
Fig. 2. Thermal decomposition of 30 mg $\text{Ce}_2(\text{CO}_3)_3 \cdot 4.5\text{H}_2\text{O}$ in (a) helium and (b) hydrogen. Heating rate: 10°C/min, detected gases: H_2O ($m/e = 18$), CO ($m/e = 28$), CO_2 ($m/e = 44$) and CH_4 ($m/e = 16$).

of CO and H₂O was also observed, probably due to the water–gas shift reaction



CO is the main product during the second part of the last step in both cases, and cannot be explained by the water–gas shift reaction. Reduction of CO₂ by Ce(III) is more probable. Since CO₂ is also evolved during the final stage of decomposition, it must be assumed that non-stoichiometric CeO_{2-x} is left as the solid product.

The reaction sequence in helium or hydrogen is then close to:



Both parts of the last decomposition step in hydrogen or helium are much more endothermic than is the last step in the presence of oxygen. The heat of decomposition is in this case much less offset by the heat of oxidation of Ce(III), because oxidation by CO₂ is less exothermic than oxidation by O₂ (table 2).

Compared to decompositions of alkaline earth carbonates [5], the lower decomposition temperatures in oxidising rather than in reducing atmosphere are surprising. A reasonable explanation is that the driving force for the decomposition is the formation of cerium(IV) oxide, which proceeds more readily in the presence of oxygen.

3.1.3. Decomposition of Rh impregnated cerium carbonate hydrate

The decomposition reactions of Rh impregnated cerium carbonate in helium and hydrogen are shown in fig. 3. Since the sample had been dried at 150°C during preparation, most crystal water of the original carbonate hydrate had been lost in the drying process. The evolution of chlorine or hydrochloric acid could not be detected in either atmosphere, indicating that the chloride introduced into the system in the impregnation step had been largely removed with the water during the drying process.

Decomposition in helium shows a series of poorly resolved endothermic processes (fig. 3a). Below 200°C, mainly H₂O is evolved. The loss of water continues up to much higher temperatures than with the pure carbonate, possibly due to the presence of hydroxides formed during impregnation. The evolution of CO₂ starts at about 200°C and maximises at 460°C, about 20°C lower than for the pure carbonate. No additional decomposition step with formation of carbon monoxide could be observed with this sample (the peak in the *m/e* = 28 curve is again due to fragmentation of CO₂ in the mass spectrometer). However, formation of hydrogen is evident from the *m/e* = 2 curve during the last decomposition step. We conclude

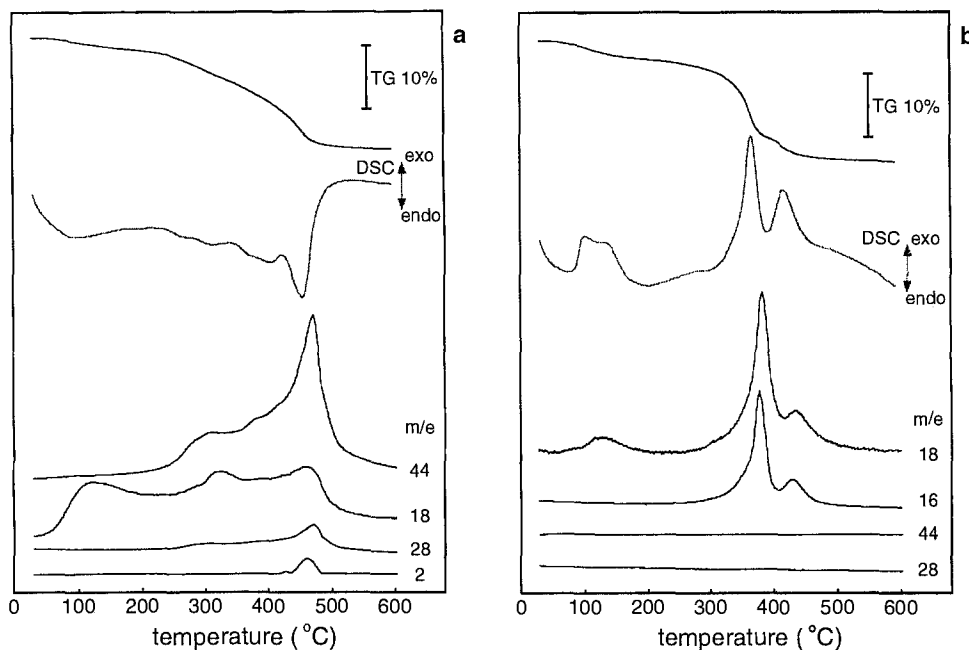
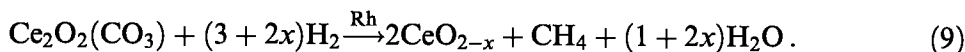
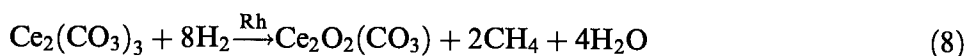


Fig. 3. Thermal decomposition of 25 mg of Rh-impregnated cerium(III) carbonate hydrate in (a) helium and (b) hydrogen. Heating rate: $10^{\circ}\text{C}/\text{min}$, detected gases: H_2 ($m/e = 2$), CH_4 ($m/e = 16$), H_2O ($m/e = 18$), CO ($m/e = 28$) and CO_2 ($m/e = 44$).

that either Ce(III) is oxidised by H_2O instead of CO_2 , or that the CO and H_2O evolved simultaneously react to form $\text{CO}_2 + \text{H}_2$ as a result of the water-gas shift activity of Rh/ceria.

During decomposition in hydrogen, three exothermic steps were observed (fig. 3b). The first one shows a doublet in the DSC curve and yields only water. It is assigned to reduction of the Rh^{3+} by hydrogen. The doublet in the DSC may originate from reduction of Rh^{3+} situated on different sites on the carbonate. During the second and third exothermic step, mixtures of H_2O and CH_2 ($m/e = 16$) are evolved. It is not possible that the signal at $m/e = 16$ results mainly from the fragmentation of water, since the intensity ratio for $m/e = 16$ to $m/e = 18$ was two orders of magnitude higher than that recorded for water alone, and because CH_3^+ fragments ($m/e = 15$) formed from CH_4 were detected simultaneously at a similar intensity. Methanation of carbon oxides proceeds quantitatively during decomposition of the carbonate in hydrogen (no CO or CO_2 was detected), in good agreement with findings for the Rh/ CaCO_3 system [5]. It was surprising to find that this part of the decomposition takes place as a two-step process. This is again attributed to the oxidation of Ce(III) to Ce(IV) that must take place in order to form the solid product CeO_{2-x} . Assuming a stoichiometry of $\text{Ce}_2(\text{CO}_3)_3$ before the last two steps, the reaction sequence can be represented by



The overall exothermic character of the reactions is due to the strong exothermicity of methanation of both CO_2 and CO (table 2).

Comparing the reaction sequences for the pure and the impregnated carbonate in helium and hydrogen atmospheres, we conclude, in agreement with suggestions of Peterson et al. [9], that an oxycarbonate “ $\text{Ce}_2\text{O}_2(\text{CO}_3)$ ” is a relatively stable intermediate in cerium carbonate decompositions in non-oxidising atmospheres. The stability of the intermediate is attributable to the fact that its decomposition must involve at least partial oxidation of Ce(III) to Ce(IV) in order to form a fluorite type oxide.

3.2. XPS MEASUREMENTS

The degradation processes of cerium carbonate hydrate in different atmospheres were also monitored by XPS, with the aim of detecting changes in the oxidation state of the cerium. Comparison of XPS and TG/MS results is limited because treatment of the samples in the preparation chamber of the XPS although similar, can never be identical to those during TG experiments, and because TG results always cover bulk properties while XPS is limited to surface and near surface regions of the sample.

The 3d spectra of Ce(III) and Ce(IV) exhibit complicated features due to shake-up and shake-down processes which have been extensively investigated both theoretically and experimentally [14–16]. For qualitative determination of Ce(III) versus Ce(IV) it is sufficient to recognise that strong peaks at $E_B = 886.2$ eV and $E_B = 904.7$ eV (labelled with v' and u' respectively) are typical for Ce(III) while the main features of Ce(IV) are at $E_B = 883.2$ eV (v), 889.2 eV (v''), 889.1 eV (v'''), 901.2 eV (u), 908.2 eV (u''), and 917.3 eV (u''').

Fig. 4 shows Ce 3d, O 1s, and C 1s spectra at different stages of the decomposition of cerium carbonate under an atmospheric pressure of oxygen. The Ce 3d spectrum of the parent material clearly shows all features of Ce(III), but also a quite strong u''' peak which is due to near surface oxidation to Ce(IV). The corresponding O 1s peak has its maximum at 531.5 eV (typical for carbonates) and a weak shoulder at 529.0 eV, which could originate from surface oxide. In the C 1s region a doublet is present. The main peak at 289.1 eV originates from carbon in carbonate and the secondary peak at 284.6 eV from adventitious carbon.

Upon heating to 200°C in oxygen, the Ce(IV) features in the Ce 3d spectrum are increased, the “oxide” shoulder in the O 1s region gains relative intensity and the carbonate loses intensity. All these changes indicate the start of decomposition to CeO_2 . When heated to 400°C, the Ce(III) features are lost. The O 1s region

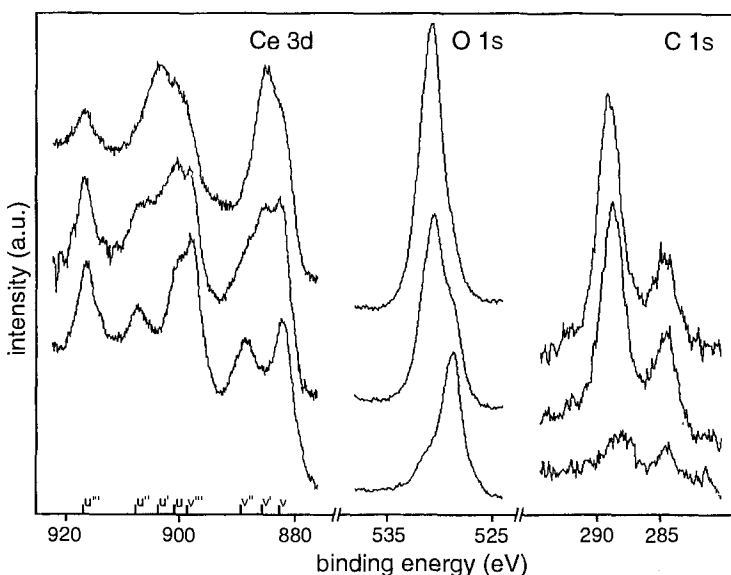


Fig. 4. XPS Ce 3d, O 1s and C 1s spectra of $\text{Ce}_2(\text{CO}_3)_3 \cdot 4.5\text{H}_2\text{O}$ (top) and of the products of reaction with oxygen for 10 min at 200°C (middle) and 400°C (bottom).

now shows predominantly oxidic character. The tailing in the high binding energy side of the spectrum is interpreted as remaining surface hydroxide and/or carbonate. Traces of remaining carbonate are also evident from the spectrum of the C 1s region.

Fig. 5 shows spectra of the carbonate after decomposition in vacuum, and after subsequent oxidation by exposure to air for 5 h. When decomposed in vacuum, Ce(III) remains the predominant oxidation state, although an increase of Ce(IV) peaks compared to the parent material is observed. The O 1s peak indicates almost complete decomposition of the carbonate. In the C 1s region the peak at 284.6 eV was found to have grown far over normal levels of adventitious carbon. This is interpreted as reduction of carbonate to graphite-like elemental carbon. This interpretation is confirmed by the colour of the sample, which had turned grey during the thermal treatment whereas cerium carbonate decomposed in air is white to pale yellow.

When ambient air was admitted to the sample, oxidation to Ce(IV) occurred, as indicated by the Ce 3d spectrum. Interaction with moisture and CO_2 at the surface yields surface carbonate and hydroxide, as indicated by the gain in relative intensity on the high binding energy side of both the C 1s and O 1s peaks.

Sample charging

All the spectra presented in this work have been corrected for electrical charging during the XPS process. For non-conducting powder samples directly dispersed

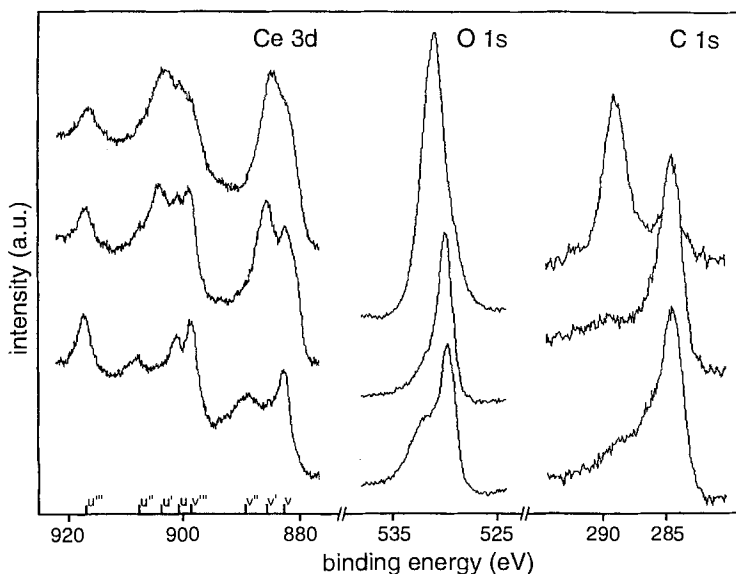


Fig. 5. XPS Ce 3d, O 1s and C 1s spectra of $\text{Ce}_2(\text{CO}_3)_3 \cdot 4.5\text{H}_2\text{O}$ (top) and of the products of decomposition in vacuum for 10 min at 500°C (middle) and after subsequent exposure to air for 5 h at room temperature (bottom).

on the stainless steel sample holders, shifts of 4–6 eV due to charging are typical in our equipment and were found for the parent material and the products of decomposition in oxygen. For the sample decomposed under vacuum the charging was only about 0.2 eV. Similar effects were found when CeO_2 impregnated with precious metals was reduced in hydrogen to form $\text{PM}/\text{CeO}_{2-x}$. The reduced sample charging indicates a relatively high conductivity, which is typical of oxygen deficient ceria. A charging of 4–6 eV is normally re-established after reoxidation of the ceria. After oxidation of the decomposed cerium carbonate by air however, the charging was slightly increased, but still below 0.5 eV. The remaining conductivity is probably due to the elemental carbon remaining in this sample.

4. Conclusions

The decomposition of cerium(III) carbonate hydrate proceeds by a large variety of different paths depending on surrounding atmospheres and admixed precious metal. Most important is the fact that the final decomposition to stoichiometric or oxygen deficient ceria must involve oxidation of Ce(III) to Ce(IV). In the presence of oxygen, this is readily done by the surrounding gas, and the decomposition temperature is relatively low. In hydrogen or helium however, the carbon dioxide or water formed are the only oxidising agents available. Since the oxidation of Ce(III) by H_2O or CO_2 needs a higher activation energy and is much less exothermic than

oxidation by O₂, the decomposition takes place at considerably higher temperatures in non-oxidising atmospheres.

The Rh/CeO_{2-x} left after decomposition of the Rh-impregnated carbonate shows catalytic activity towards the water-gas shift reaction as well as towards methanation of carbon monoxide and carbon dioxide. This may be important for various applications in heterogeneous catalysis, but especially for car exhaust systems, where combinations of Rh and ceria are widely used, and hydrogen, water, and carbon oxides are involved in the catalytic reactions.

Acknowledgement

This study was supported by the Swiss National Science Foundation. Thanks are due to Scott Buckingham for assistance with the TG/MS measurements.

References

- [1] B. Harrison, A.F. Diwell and C. Hallett, *Platinum Met. Rev.* 32 (1988) 73.
- [2] C. Padeste, N.W. Cant and D.L. Trimm, *Catal. Lett.* 18 (1993) 305.
- [3] N. Afify, A.S. Abdel-Halim and S.M. El-Hout, *J. Thermal Anal.* 34 (1988) 198.
- [4] S.H. Oh and C.C. Eickel, *J. Catal.* 112 (1988) 543.
- [5] C. Padeste, A. Reller and H.R. Oswald, *Mater. Res. Bull.* 25 (1990) 1299.
- [6] A. Tsuneto, A. Kudo, N. Saito and T. Sakata, *Chem. Lett.* (1992) 831.
- [7] R. Emmenegger, H.R. Oswald and A. Reller, *Solar Energy Mater.* 24 (1991) 397.
- [8] M.N. Ambrozhi, E.F. Luchnikova and M.I. Sidorova, *Russ. J. Inorg. Chem.* 5 (1960) 176.
- [9] E.J. Peterson, E.I. Onstott, M.R. Johnson and M.G. Bowman, *J. Inorg. Nucl. Chem.* 40 (1978) 1357.
- [10] I. Barin, O. Knacke and O. Kubaschewski, *Thermochemical Properties of Inorganic Substances* (Springer, Berlin, 1977).
- [11] M.Kh. Karapet'yants and M.L. Karapet'yants, *Thermodynamic Constants of Inorganic and Organic Compounds* (Humphrey Science Publishers, London, 1970).
- [12] A. Fujimori, *Phys. Rev. B* 28 (1983) 2281.
- [13] G. Praline, B.E. Koel, R.L. Hance, H.-I. Lee and J.M. White, *J. Electron Spectry. Rel. Phenom.* 21 (1980) 21.
- [14] F. Le Normand, J. El Fallah, L. Hilaire, P. Légaré, A. Kotani and J.C. Parlebas, *Solid State Commun.* 71 (1989) 885.